



Deposited via The University of Leeds.

White Rose Research Online URL for this paper:

<https://eprints.whiterose.ac.uk/id/eprint/206725/>

Version: Accepted Version

Article:

Jerez, D.J., Fragkoulis, V.C., Ni, P. et al. (2024) Operator norm-based determination of failure probability of nonlinear oscillators with fractional derivative elements subject to imprecise stationary Gaussian loads. *Mechanical Systems and Signal Processing*, 208. 111043. ISSN: 0888-3270

<https://doi.org/10.1016/j.ymssp.2023.111043>

© 2023, Elsevier. This manuscript version is made available under the CC-BY-NC-ND 4.0 license <http://creativecommons.org/licenses/by-nc-nd/4.0/>.

Reuse

This article is distributed under the terms of the Creative Commons Attribution-NonCommercial-NoDerivs (CC BY-NC-ND) licence. This licence only allows you to download this work and share it with others as long as you credit the authors, but you can't change the article in any way or use it commercially. More information and the full terms of the licence here: <https://creativecommons.org/licenses/>

Takedown

If you consider content in White Rose Research Online to be in breach of UK law, please notify us by emailing eprints@whiterose.ac.uk including the URL of the record and the reason for the withdrawal request.



Operator norm-based determination of failure probability of nonlinear oscillators with fractional derivative elements subject to imprecise stationary Gaussian loads

D. J. Jerez ^a, V. C. Fragkoulis ^{b,1}, P. Ni ^c, I. P. Mitseas ^{d,e}, M. A. Valdebenito ^f,
M. G. R. Faes ^f, and M. Beer ^{c,g,h}

^a *Departamento de Ingeniería Civil, Universidad Técnica Federico Santa María, Avda. España 1680, Valparaíso 2390123, Chile*

^b *Department of Civil and Environmental Engineering, University of Liverpool, Liverpool L69 3GH, UK*

^c *Institute for Risk and Reliability, Leibniz Universität Hannover, Callinstr. 34, Hannover 30167, Germany*

^d *School of Civil Engineering, University of Leeds, Leeds LS2 9JT, UK*

^e *School of Civil Engineering, National Technical University of Athens, Iroon Polytechniou 9, Zografou 15780, Greece*

^f *Chair for Reliability Engineering, TU Dortmund University, Leonard-Euler Straße 5, Dortmund 44227, Germany*

^g *Institute for Risk and Uncertainty and School of Engineering, University of Liverpool, Liverpool L69 7ZF, UK*

^h *International Joint Research Center for Resilient Infrastructure & International Joint Research Center for Engineering Reliability and Stochastic Mechanics, Tongji University, Shanghai 200092, China*

Abstract

An approximate analytical technique is developed for bounding the first-passage probability of lightly damped nonlinear and hysteretic oscillators endowed with fractional derivative elements and subjected to imprecise stationary Gaussian loads. In particular, the statistical linearization and stochastic averaging methodologies are integrated with an operator norm-based approach to formulate a numerically efficient proxy for the first-passage probability. This proxy is employed to determine the realizations of the interval-valued parameters of the excitation model that yield the extrema of the failure probability function. Ultimately, each failure probability bound is determined in a fully decoupled manner by solving a standard optimization problem followed by a single evaluation of the first-passage probability.

¹vasileios.fragkoulis@liverpool.ac.uk

The proposed approximate technique can be construed as an extension of a recently developed operator norm scheme to account for oscillators with fractional derivative elements. In addition, it can readily treat a wide range of nonlinear and hysteretic behaviors. To illustrate the applicability and effectiveness of the proposed technique, a hardening Duffing and a bilinear hysteretic nonlinear oscillators with fractional derivative elements subject to imprecise stationary Gaussian loads are considered as numerical examples.

Keywords: Uncertainty quantification, First-passage probability, Imprecise probabilities, Fractional derivative, Stochastic averaging, Statistical linearization

1 Introduction

Stochastic excitation models furnish a versatile probabilistic tool to assess the effect of uncertain dynamic loads on structural systems [1–4], where Gaussian processes have been employed in numerous engineering applications [5–7]. In this setting, the first-passage probability [8] constitutes a suitable performance measure for structural dynamical systems under stochastic excitation whose behavior can be classified as acceptable (safe) or unacceptable (failed). From a practical perspective, however, a crisp definition of the corresponding excitation model parameters remains challenging due to, for instance, lack of knowledge, scarce or noisy data, or conflicting evidence [9]. Thus, evaluating the effect of these parametric uncertainties on the first-passage probability is pivotal for reliability assessment purposes.

In light of this, employing interval-valued excitation model parameters represents a standard approach for developing uncertainty quantification frameworks [10]. Hence, the stochastic response process becomes interval-valued, and therefore the corresponding failure probability also becomes an interval variable [11]. Bounding the latter can be computationally demanding even for small-scale linear systems, since reliability assessment must be performed for different realizations of the interval model parameters [12]. To address this issue, several approaches have been proposed to bound first-passage probabilities (e.g., [13–16]). In the context of linear structural systems under Gaussian excitation, the operator norm-based decoupling framework proposed in [17, 18] allows estimating the failure probability bounds in a fully decoupled manner with the solution of two standard optimization problems, followed by two reliability analyses. Such an approach has been extended recently in [19] to account for nonlinear systems by resorting

to the statistical linearization method [20].

Further, fractional calculus has become the focal point of research for the efficient modeling of diverse systems [21]. In terms of engineering applications, it has been extensively used to construct, for instance, accurate models for capturing the viscoelastic behavior of materials [22, 23], or for describing the impedance of electrical systems [24]. In this regard, several approaches with different advantages and limitations have been developed to assess the stochastic response of systems endowed with fractional derivative elements (e.g., [25–29]). Nevertheless, a persisting challenge in the field of stochastic dynamics relates to determining the first-passage probability of nonlinear single-degree-of-freedom (SDOF) systems with fractional derivative elements; see, indicatively, [30–34]. To this end, methods such as stochastic averaging [35, 36] and statistical linearization [20, 37] have been proven as rather efficient and versatile tools. Their extensive use over the last decades relates to their capacity to treat systems exhibiting a wide range of nonlinear and hysteretic behaviors under diverse types of stochastic excitation (e.g., [38–40]).

In this paper, an analytical approximate technique is proposed for bounding the first-passage probability of nonlinear oscillators with fractional derivative elements and subject to stationary Gaussian loads, in which the corresponding excitation model parameters are interval-valued. Specifically, the statistical linearization and stochastic averaging methodologies are combined with the operator norm-based framework proposed in [18] to develop a numerically efficient proxy for the first-passage probability. The parameter values that yield the minimum and maximum of the proxy function are used to determine the lower and upper bounds, respectively, of the first-passage probability. Hence, the repeated evaluation of the failure probability is circumvented, and the sought bounds can be estimated in a fully decoupled manner. The proposed technique can be construed as an extension of the operator norm-based linearization scheme developed in [19] to account for systems with fractional derivative elements. Its advantage relates to the fact that it can readily treat diverse nonlinear and hysteretic behaviors while exhibiting relatively low computational cost. Two numerical examples are used to assess the efficacy of the technique. Namely, a hardening Duffing and a bilinear hysteretic nonlinear oscillators with fractional derivative elements subject to imprecise Gaussian loading are considered, while comparisons with reference values computed by a direct double-loop implementation are used to validate the obtained results.

2 Problem description

2.1 Nonlinear oscillator with fractional derivative elements

The governing equation of motion of a class of stochastically excited nonlinear oscillators endowed with fractional derivative elements is given by

$$\ddot{x}(t) + \beta D_{0,t}^\alpha x(t) + g(x, \dot{x}) = q(t), \quad (1)$$

where x denotes the response displacement and a dot over a variable accounts for time differentiation. Further, β is a constant damping coefficient, $g(x, \dot{x})$ is an arbitrary nonlinear function that can account also for hysteretic response behaviors, and $q(t)$ represents the system excitation modeled as a zero-mean stationary Gaussian process described by the power spectrum $S_{qq}(\omega)$. Finally, $D_{0,t}^\alpha(\cdot)$ denotes the Caputo fractional derivative operator of order α defined as [21]

$$D_{0,t}^\alpha x(t) = \frac{1}{\Gamma(1-\alpha)} \int_0^t \frac{\dot{x}(\tau)}{(t-\tau)^\alpha} d\tau, \quad (2)$$

where $0 < \alpha < 1$ and $\Gamma(\cdot)$ denotes the Gamma function.

2.2 Interval-valued first-passage probability

Choosing appropriate model parameter values in Eq. (1) is usually associated with considerable uncertainty levels due to, for instance, lack of knowledge or conflicting evidence [9]. To address this issue, it is often preferred to represent these parameters using the so-called non-traditional models for uncertainty quantification [10]. In this regard, assume that a set of parameters $\boldsymbol{\theta} \in \mathbb{R}^{n_\theta}$ associated with the excitation model are represented as interval variables. That is, they are bounded by the hyper-rectangle

$$\Theta = \{ \boldsymbol{\theta} \in \mathbb{R}^{n_\theta} : \theta_i^L \leq \theta_i \leq \theta_i^U, i = 1, 2, \dots, n_\theta \}, \quad (3)$$

where θ_i^L and θ_i^U denote, respectively, the lower and upper bounds between which the true value for the i -th parameter is expected to lie. Note that, in this setting, the power spectrum of the excitation process satisfies $S_{qq}(\omega) = S_{qq}(\omega, \boldsymbol{\theta})$. Hence, Eq. (1) involves both random and interval variables, and thus, the dynamic response becomes an interval stochastic process [10]. This must be properly accounted for to assess the performance of the corresponding oscillator.

The first-passage probability [8], denoted as P_F , constitutes a suitable measure of performance when the structural behavior can be qualified as acceptable or unacceptable. Specifically, the corresponding first-passage event is defined as

$$F = \max_{t \in [0, T]} \max_{\ell=1,2,\dots,n_h} \left| \frac{h_\ell(t)}{h_\ell^*} \right| > 1, \quad (4)$$

where T denotes the simulation period and $h_\ell(t)$, $\ell = 1, 2, \dots, n_h$, are the responses of interest with corresponding thresholds $h_\ell^* > 0$. Thus, failure occurs when the magnitude of any response of interest obtained by solving Eq. (1) exceeds its maximum allowable level at any instant of the simulation period. In this context, the first-passage probability can be explicitly defined as

$$P_F = P(h_\ell(t) > h_\ell^* \text{ for some } t \in [0, T] \text{ and some } \ell \in \{1, 2, \dots, n_h\}), \quad (5)$$

where $P(\cdot)$ denotes the probability of the event inside the parentheses. Since the interval-valued parameters $\boldsymbol{\theta}$ affect the characteristics of the stochastic excitation, then $P_F(\boldsymbol{\theta}) = P(F|\boldsymbol{\theta})$. Moreover, the first-passage probability satisfies [10]

$$P_F(\boldsymbol{\theta}) \in [P_F^L, P_F^U] = \left[\min_{\boldsymbol{\theta} \in \Theta} P_F(\boldsymbol{\theta}), \max_{\boldsymbol{\theta} \in \Theta} P_F(\boldsymbol{\theta}) \right], \quad (6)$$

where P_F^L and P_F^U denote the lower and upper bounds of $P_F(\boldsymbol{\theta})$, respectively. Therefore, the evaluation of the bounds for $P_F(\boldsymbol{\theta})$ involves, in principle, the solution of two optimization problems with the failure probability as objective function. A straightforward solution treatment leads to the so-called double-loop approaches, where reliability analysis is performed in the inner loop and the outer loop comprises an optimization procedure (with respect to the parameters $\boldsymbol{\theta}$) [12].

3 Proposed linearization framework to bound first-passage probabilities

While the bounds on the first-passage probability in Eq. (6) provide valuable information for decision-making processes, their direct determination using double-loop approaches often proves computationally challenging [11]. To address this issue, a novel approach has been proposed in [19] by combining the statistical linearization method [20] with an operator norm-based solution treatment [17]. In this setting, the computationally demanding problem of bounding the first-passage

failure probability of a class of nonlinear structural systems under Gaussian excitation has been simplified significantly. Specifically, each bound in Eq. (6) can be computed by considering a single deterministic optimization problem in conjunction with a single reliability analysis. Building on some of the previous ideas, an approximate analytical technique based on the integration of the statistical linearization and stochastic averaging methodologies with an operator norm-based decoupling framework is proposed next to account for nonlinear oscillators with fractional derivative elements.

3.1 Equivalent linear oscillator determination

For a given realization of the interval parameters θ , and considering that the oscillator in Eq. (1) is lightly damped, its response follows a pseudo-harmonic behavior described by [20, 41]

$$x(t) = A(t) \cos(\omega(A)t + \psi(t)) \quad (7)$$

and

$$\dot{x}(t) = -\omega(A)A(t) \sin(\omega(A)t + \psi(t)). \quad (8)$$

In Eqs. (7) and (8), $\omega(A)$ denotes the amplitude-dependent natural frequency, and $A(t)$ and $\psi(t)$ correspond to the response amplitude and phase, respectively. These are considered as slowly-varying with respect to time processes, and thus, constant over one cycle of oscillation [20]. Therefore, assuming that $A(t) = A$ and $\psi(t) = \psi$, and manipulating Eqs. (7) and (8) leads to

$$A^2 = x^2(t) + \left(\frac{\dot{x}(t)}{\omega(A)} \right)^2. \quad (9)$$

Next, Eq. (1) is written for simplicity as [32]

$$\ddot{x}(t) + \beta_0 \dot{x}(t) + g_0(x, \dot{x}) = q(t), \quad (10)$$

where

$$g_0(x, \dot{x}) = \beta D_{0,t}^\alpha x + g(x, \dot{x}) - \beta_0 \dot{x}. \quad (11)$$

In Eq. (11), $\beta_0 = 2\zeta_0\omega_0$, where ω_0 and ζ_0 denote the natural frequency and damping ratio of the corresponding linear oscillator. Further, applying a statistical linearization treatment, Eq. (10) is approximated by the equivalent linear oscillator [20, 41, 42]

$$\ddot{x}(t) + (\beta_0 + \beta(A)) \dot{x}(t) + \omega^2(A)x(t) = q(t), \quad (12)$$

where $\beta(A)$ and $\omega^2(A)$ denote the amplitude-dependent equivalent elements of the linearized system. For the determination of the equivalent elements, the difference between Eqs. (10) and (12) is formulated and minimized in the mean-square sense over one cycle of oscillation [20]. This leads to

$$\beta(A) = \frac{\omega_0^2}{A\omega(A)} F_1(A) + \frac{\beta}{\omega^{1-\alpha}(A)} \sin\left(\frac{\alpha\pi}{2}\right) - \beta_0 \quad (13)$$

and

$$\omega^2(A) = \frac{\omega_0^2}{A} F_2(A) + \beta\omega^\alpha(A) \cos\left(\frac{\alpha\pi}{2}\right), \quad (14)$$

with

$$F_1(A) = -\frac{1}{\pi} \int_0^{2\pi} g(A \cos \phi, -A\omega(A) \sin \phi) \sin \phi d\phi, \quad (15)$$

$$F_2(A) = \frac{1}{\pi} \int_0^{2\pi} g(A \cos \phi, -A\omega(A) \sin \phi) \cos \phi d\phi \quad (16)$$

and $\phi = \omega(A)t + \psi$. The interested reader is directed to [32, 38, 41] for a detailed derivation of Eqs. (10)-(16).

The amplitude-dependent equivalent elements in Eqs. (13) and (14) are then approximated by corresponding time-dependent equivalent elements. Specifically, taking expectations on Eqs. (13) and (14), the equivalent elements are given by [20]

$$\beta_{eq} = \int_0^\infty \beta(A)p(A)dA \quad (17)$$

and

$$\omega_{eq}^2 = \int_0^\infty \omega^2(A)p(A)dA, \quad (18)$$

where $p(A)$ denotes the response amplitude probability density function (PDF). In this context, the equivalent linear system in Eq. (12) becomes

$$\ddot{x}(t) + (\beta_0 + \beta_{eq})\dot{x}(t) + \omega_{eq}^2 x(t) = q(t). \quad (19)$$

Clearly, the response amplitude PDF is required for the computation of β_{eq} and ω_{eq}^2 in Eqs. (17) and (18). Thus, following the standard stochastic averaging method, the stochastic differential equation governing the slowly varying response

amplitude process is constructed, and the associated Fokker-Planck equation is formulated (e.g., [35])

$$\begin{aligned} \frac{\partial p(A)}{\partial t} = & -\frac{\partial}{\partial A} \left\{ \left(-\frac{1}{2}(\beta_0 + \beta_{eq})A + \frac{\pi S_{qq}(\omega_{eq})}{2\omega_{eq}^2 A} \right) p(A) \right\} \\ & + \frac{1}{4} \frac{\partial}{\partial A} \left\{ \frac{\pi S_{qq}(\omega_{eq})}{\omega_{eq}^2} \frac{\partial p(A)}{\partial A} + \frac{\partial}{\partial A} \left(\frac{\pi S_{qq}(\omega_{eq})}{\omega_{eq}^2} p(A) \right) \right\}. \end{aligned} \quad (20)$$

Notably, for the general case of linear systems subject to stationary excitation, i.e., when $\frac{\partial p(A)}{\partial t} = 0$, a straightforward solution of Eq. (20) is readily available in the form of a Rayleigh distribution (e.g., [43, 44]). This result has been recently extended in [45] and a closed-form expression for the response amplitude PDF $p(A)$ corresponding to oscillators with fractional derivative elements has been proposed. This has the form

$$p(A) = \frac{\sin\left(\frac{\alpha\pi}{2}\right) A}{\omega_0^{1-\alpha} \sigma^2} \exp\left(-\frac{\sin\left(\frac{\alpha\pi}{2}\right) A^2}{\omega_0^{1-\alpha} 2\sigma^2}\right), \quad (21)$$

where

$$\sigma^2 = \frac{\pi S_{qq}(\omega_{eq})}{(\beta_0 + \beta_{eq})\omega_{eq}^2}. \quad (22)$$

In passing, it is noted that Eqs. (21) and (22) have been further generalized to account for both standard oscillators and oscillators with fractional derivative elements subject to non-stationary excitation; the interested reader is directed to [27, 33, 40, 42, 44] for a relevant discussion.

3.2 Operator norm-based solution treatment

To exploit the linearity of the equivalent oscillator given by Eq. (19), an operator norm-based solution treatment [17, 19] is implemented for determining the failure probability bounds in Eq. (6). Without loss of generality, the zero-mean discrete Gaussian load in Eq. (19) is modeled by adopting the Karhunen-Loève expansion [46]. Specifically,

$$q(t_k, \boldsymbol{\theta}, \boldsymbol{\xi}) = \boldsymbol{\psi}_k^T(\boldsymbol{\theta})\boldsymbol{\xi}, \quad (23)$$

$k = 1, 2, \dots, n_T$, represents the loading at time $t_k = (k-1)\Delta t$, where Δt denotes the time step, $n_T = T/\Delta t + 1$ is the number of time instants, and $\boldsymbol{\xi} \in \mathbb{R}^{n_\xi}$ is a standard Gaussian random variable vector. Further, $\boldsymbol{\psi}_k(\boldsymbol{\theta})$ corresponds to the k -th column of the matrix $\boldsymbol{\Psi}(\boldsymbol{\theta}) = \boldsymbol{\Lambda}^{1/2}(\boldsymbol{\theta})\boldsymbol{\Upsilon}^T(\boldsymbol{\theta})$, where $\boldsymbol{\Lambda}(\boldsymbol{\theta})$ denotes the diagonal

$n_\xi \times n_\xi$ matrix comprising the n_ξ largest eigenvalues of the stochastic load covariance matrix $\Sigma(\boldsymbol{\theta})$, and $\Upsilon(\boldsymbol{\theta})$ denotes the $n_T \times n_\xi$ matrix of the corresponding eigenvectors, i.e., $\Sigma(\boldsymbol{\theta})\Upsilon(\boldsymbol{\theta}) = \Upsilon(\boldsymbol{\theta})\Lambda(\boldsymbol{\theta})$.

Next, assume that the vector containing the n_T discrete values of the ℓ -th normalized response of interest is defined as

$$\bar{\mathbf{h}}_\ell(\boldsymbol{\theta}, \boldsymbol{\xi}) = \frac{1}{h_\ell^*} [h_\ell(t_1, \boldsymbol{\theta}, \boldsymbol{\xi}) \quad \dots \quad h_\ell(t_{n_T}, \boldsymbol{\theta}, \boldsymbol{\xi})]^\top, \quad (24)$$

for $\ell = 1, 2, \dots, n_h$. Further, defining the vector

$$\bar{\mathbf{h}}(\boldsymbol{\theta}, \boldsymbol{\xi}) = [\bar{\mathbf{h}}_1^\top(\boldsymbol{\theta}, \boldsymbol{\xi}) \quad \dots \quad \bar{\mathbf{h}}_{n_h}^\top(\boldsymbol{\theta}, \boldsymbol{\xi})]^\top, \quad (25)$$

and since the equivalent oscillator in Eq. (19) enables a linear relationship between the system response and the excitation, a linear relationship between the responses of interest at discrete time instants and the basic random variables is also established as [47, 48]

$$\bar{\mathbf{h}}(\boldsymbol{\theta}, \boldsymbol{\xi}) = \mathbf{M}(\boldsymbol{\theta})\boldsymbol{\xi}. \quad (26)$$

In Eq. (26), $\mathbf{M}(\boldsymbol{\theta}) \in \mathbb{R}^{n_T n_h \times n_\xi}$ is obtained in terms of the response thresholds, the matrix $\Psi(\boldsymbol{\theta})$, and the adopted integration rule for the equation of motion. The linear mapping $\mathbf{M}(\boldsymbol{\theta})$ depends on the parameters $\boldsymbol{\theta}$ since the latter affect the stochastic excitation model. In this context, the induced (p_1, p_2) -norm of $\mathbf{M}(\boldsymbol{\theta})$ is given by

$$\|\mathbf{M}(\boldsymbol{\theta})\|_{p_1, p_2} = \sup_{\boldsymbol{\xi} \neq \mathbf{0}} \frac{\|\mathbf{M}(\boldsymbol{\theta})\boldsymbol{\xi}\|_{p_1}}{\|\boldsymbol{\xi}\|_{p_2}} = \sup_{\boldsymbol{\xi} \neq \mathbf{0}} \frac{\|\bar{\mathbf{h}}(\boldsymbol{\theta}, \boldsymbol{\xi})\|_{p_1}}{\|\boldsymbol{\xi}\|_{p_2}}, \quad (27)$$

where $\|\cdot\|_{p_i}$ denotes the p_i -norm of a vector ($i = 1, 2$). Following the presentation in [17, 19], the values $p_1 = \infty$ and $p_2 = 2$ are adopted in the ensuing analysis. Thus, it can be argued that the operator norm expression in Eq. (27) quantifies the maximum amplification of the response magnitude, in terms of the maximum absolute value of the normalized responses over time, with respect to the magnitude of the input vector $\boldsymbol{\xi}$, in terms of its Euclidean distance. This choice also enables the analytical evaluation of the operator norm [49].

The key idea of the proposed framework is that the values of $\boldsymbol{\theta}$ that yield the minimum (maximum) amplification of the response magnitude will also yield the lower (upper) bound for the failure probability [17]. In other words, the function $\|\mathbf{M}(\boldsymbol{\theta})\|_{p_1, p_2}$ is employed as a numerically efficient proxy for the failure probability function $P_F(\boldsymbol{\theta})$. Hence, the values of $\boldsymbol{\theta}$ that determine the extrema of

$\|\mathbf{M}(\boldsymbol{\theta})\|_{\infty,2}$ are employed to determine the bounds of $P_F(\boldsymbol{\theta})$ in Eq. (6). This leads to

$$[P_F^L, P_F^U] \approx [P_F(\boldsymbol{\theta}^{*,L}), P_F(\boldsymbol{\theta}^{*,U})], \quad (28)$$

where

$$\boldsymbol{\theta}^{*,L} = \underset{\boldsymbol{\theta} \in \Theta}{\operatorname{argmin}} \|\mathbf{M}(\boldsymbol{\theta})\|_{\infty,2} \quad (29)$$

and

$$\boldsymbol{\theta}^{*,U} = \underset{\boldsymbol{\theta} \in \Theta}{\operatorname{argmax}} \|\mathbf{M}(\boldsymbol{\theta})\|_{\infty,2}. \quad (30)$$

Clearly, the solution of two deterministic optimization problems to derive the parameter values that yield the extrema of the operator norm, followed by two corresponding reliability analyses, are sufficient for estimating the failure probability bounds P_F^L and P_F^U in Eq. (28). In other words, the repeated evaluation of the failure probability associated with the direct solution of Eq. (6) is bypassed by virtue of the proposed framework.

3.3 Summary of the proposed approach

The herein proposed approach comprises the following key aspects to bound the first-passage probability of nonlinear oscillators with fractional derivative elements. First, the statistical linearization and stochastic averaging methodologies are combined to determine an equivalent linear system for any given realization of the interval-valued model parameters. Based on this linearization an associated operator norm function is defined. The resulting mapping is employed as a proxy function to estimate the parameter values that determine the bounds of the first-passage probability via Eq. (28). Ultimately, the bounds in Eq. (6) are approximated in a two-step process as follows:

1. Solve Eqs. (29) and (30) to determine the parameter values $\boldsymbol{\theta}^{*,L}$ and $\boldsymbol{\theta}^{*,U}$ that yield the failure probability bounds. It is noted that the evaluation of $\|\mathbf{M}(\boldsymbol{\theta})\|_{\infty,2}$ at any given value of $\boldsymbol{\theta}$ involves two main tasks, namely, (i) finding an equivalent linear oscillator according to Section 3.1, and (ii) computing the corresponding matrix $\mathbf{M}(\boldsymbol{\theta})$ in Eq. (26). Since the function $\|\mathbf{M}(\boldsymbol{\theta})\|_{\infty,2}$ is non-smooth, suitable search algorithms must be adopted for the solution of the related optimization problems.
2. Estimate the failure probability bounds, that is, $P_F^L \approx P_F(\boldsymbol{\theta}^{*,L})$ and $P_F^U \approx P_F(\boldsymbol{\theta}^{*,U})$. This is done by considering the nonlinear oscillator in Eq. (1) in conjunction with any suitable reliability assessment method.

The proposed approach encompasses some attractive features pertaining to its practical implementation. First, the numerical cost of solving Eqs. (29) and (30) is relatively low, since evaluating the corresponding objective function is significantly less computationally intensive than estimating the corresponding first-passage failure probability. In addition, by virtue of the proposed two-step implementation, failure probability bounds are computed in a fully decoupled manner. That is, a single estimation of the failure probability by means of any suitable reliability analysis method is sufficient to determine each bound in Eq. (28). Finally, the adoption of the statistical linearization and averaging methodologies allows to treat diverse nonlinear and hysteretic response behaviors, while exhibiting low computational cost. Overall, the developed framework can be regarded as a versatile and computationally efficient alternative for bounding the first-passage probability of a class of nonlinear oscillators endowed with fractional derivative elements.

4 Numerical examples

In this section, two numerical examples are considered to assess the efficacy of the proposed framework. Specifically, first-passage probability bounds are determined for a hardening Duffing and a bilinear hysteretic nonlinear oscillators endowed with fractional derivative elements. For both examples, the load $q(t)$ in Eq. (1) is modeled as a zero-mean Gaussian stochastic process characterized by the Clough-Penzien spectrum [50]

$$S_{qq}(\omega) = \frac{\omega^4 (\omega_g^4 + (2\zeta_g \omega_g \omega)^2) S_0}{[(\omega_g^2 - \omega^2)^2 + (2\zeta_g \omega_g \omega)^2] [(\omega_f^2 - \omega^2)^2 + (2\zeta_f \omega_f \omega)^2]}, \quad (31)$$

with S_0 denoting the intensity of the excitation, ω_g and ω_f representing the natural circular frequencies of the filter, and ζ_g and ζ_f representing the corresponding damping ratios. These parameters are modeled as interval variables in the subsequent examples, with reference values given by $S_0^{\text{ref}} = 0.50$, $\omega_g^{\text{ref}} = 12.47$, $\omega_f^{\text{ref}} = 5.43$, $\zeta_f^{\text{ref}} = 0.80$ and $\zeta_g^{\text{ref}} = 0.68$.

In all cases addressed herein, the first-passage failure event is defined in terms of the displacement response $x(t)$ as

$$F = \max_{t \in [0, T]} \frac{|x(t)|}{x^*} > 1, \quad (32)$$

where $T = 18$ s is the reference period and x^* is the maximum admissible displacement level. Further, a time step of $\Delta t = 0.03$ s is assumed. For illustration

purposes, the entire set of eigenvalues of the covariance matrix is considered in Eq. (23). Therefore, the discrete representation of the stochastic excitation involves a total of $n_\xi = 601$ random variables for the examples in the ensuing analysis. It is noted that alternative responses of interest, such as the oscillator velocity or acceleration, can also be considered in the definition of the failure event F in Eq. (32).

Following the presentation in Section 3, the implementation of the herein proposed approach requires the solution of Eqs. (29) and (30). In particular, the stochastic search technique presented in [51] is adopted to this end. The latter has proved rather effective to address a class of optimization problems involving structural dynamical systems under stochastic excitation. Nevertheless, alternative optimization schemes can also be implemented to determine $\theta^{*,L}$ and $\theta^{*,U}$. Further, first-passage probabilities are evaluated using subset simulation [52, 53], a well-established reliability analysis method. Specifically, failure probability estimates are obtained by averaging the results of ten independent subset simulation runs with 2000 samples per stage each. The number of independent runs and samples per stage can be certainly reduced for practical implementation purposes. Moreover, alternative reliability analysis methods can also be implemented. Finally, reference values for the failure probability bounds are obtained using a direct double-loop approach that employs the stochastic optimization method in [51] to find the extrema of $P_F(\theta)$, subset simulation [52] for estimating the first-passage probability corresponding to the oscillator in Eq. (1), and the customary strategy of employing the same sequence of pseudorandom numbers to evaluate the failure probability at different realizations of the interval-valued parameters [54].

4.1 Duffing nonlinear oscillator with fractional derivative elements

In this section, a hardening Duffing nonlinear oscillator with fractional derivative elements is considered. Specifically, the nonlinear function in Eq. (1) is defined as

$$g(x, \dot{x}) = \omega_0^2 x (1 + \varepsilon x^2), \quad (33)$$

where $\varepsilon > 0$ is a constant controlling the magnitude of the nonlinearity. Next, following the presentation in Section 3, the equivalent linear oscillator in Eq. (19) is determined for any given value of the interval parameter vector θ . Taking into account the nonlinear function given by Eq. (33), the quantities $F_1(A)$ and $F_2(A)$ are computed from Eqs. (15) and (16), respectively. This, in turn, allows determining the amplitude-dependent equivalent element $\beta(A)$ and $\omega^2(A)$ in Eqs. (13) and (14). These expressions are then substituted into Eqs. (17) and (18) which, in

conjunction with the stationary response amplitude PDF given by Eq. (21), lead to

$$\beta_{eq} = -\beta_0 + \frac{\beta \sin^2\left(\frac{\alpha\pi}{2}\right)}{\omega_0^{1-\alpha}\sigma^2} \int_0^\infty \frac{A}{\omega^{1-\alpha}(A)} \exp\left(-\frac{\sin\left(\frac{\alpha\pi}{2}\right) A^2}{\omega_0^{1-\alpha} 2\sigma^2}\right) dA \quad (34)$$

and

$$\begin{aligned} \omega_{eq}^2 = & \omega_0^2 + \frac{\beta \sin\left(\frac{\alpha\pi}{2}\right) \cos\left(\frac{\alpha\pi}{2}\right)}{\omega_0^{1-\alpha}\sigma^2} \int_0^\infty A\omega^\alpha(A) \exp\left(-\frac{\sin\left(\frac{\alpha\pi}{2}\right) A^2}{\omega_0^{1-\alpha} 2\sigma^2}\right) dA \\ & + \frac{3\varepsilon\omega_0^{1+\alpha} \sin\left(\frac{\alpha\pi}{2}\right)}{4\sigma^2} \int_0^\infty A^3 \exp\left(-\frac{\sin\left(\frac{\alpha\pi}{2}\right) A^2}{\omega_0^{1-\alpha} 2\sigma^2}\right) dA, \end{aligned} \quad (35)$$

respectively. Clearly, Eqs. (34), (35) and Eq. (22) define a coupled system of nonlinear algebraic equations to be solved for determining the equivalent elements β_{eq} and ω_{eq}^2 . This is done by resorting to the simple iterative scheme described in Appendix A. Nevertheless, alternative solution strategies can also be adopted.

In the ensuing analysis, the system parameter values in Eqs. (1) and (33) are $\alpha = 0.5$, $\omega_0 = 10$, $\beta = 2\zeta_0\omega_0^{2-\alpha} = 6.32$ with $\zeta_0 = 0.1$, and $\varepsilon = 2$. In addition, the response threshold in Eq. (32) is $x^* = 0.37$.

4.1.1 Case I: Clough-Penzien spectrum with two interval-valued parameters

First, for demonstration purposes, the following values are considered for the parameters of the Clough-Penzien spectrum in Eq. (31): $S_0 = S_0^{\text{ref}}\theta_1$, $\omega_f = \omega_f^{\text{ref}}\theta_2$, $\zeta_f = \zeta_f^{\text{ref}}\theta_2$, $\omega_g = \omega_g^{\text{ref}}$ and $\zeta_g = \zeta_g^{\text{ref}}$, where θ_1 and θ_2 are interval variables such that $0.8 \leq \theta_i \leq 1.2$, $i = 1, 2$. Thus, it is assumed that ω_g and ζ_g are equal to their reference values, whereas the parameters S_0 , ω_f and ζ_f are bounded between 80% and 120% of their corresponding reference values.

The key idea of the herein proposed framework is to employ the operator norm $\|\mathbf{M}(\boldsymbol{\theta})\|_{\infty,2}$ defined in Eq. (27), which is associated with the equivalent linear oscillator corresponding to the excitation model defined by $\boldsymbol{\theta}$, as a numerically efficient proxy for the failure probability function. That is, $P_F(\boldsymbol{\theta})$ is evaluated at the parameter values that minimize (maximize) $\|\mathbf{M}(\boldsymbol{\theta})\|_{\infty,2}$ in order to obtain the lower (upper) bound of the first-passage probability. In this regard, Fig. 1 shows the contours of $P_F(\boldsymbol{\theta})$ and $\|\mathbf{M}(\boldsymbol{\theta})\|_{\infty,2}$, which have been generated by evaluating both functions at different values of $\boldsymbol{\theta}$ distributed over $[0.8, 1.2]^2$. The resulting

curves for the failure probability function, which are fairly rugged due to the inherent variability of sampling-based estimates, have been smoothed to provide a more clear representation of the function behavior. It is seen that an increase in θ_1 can be compensated by a decrease in θ_2 to maintain the same failure probability level, and a similar behavior holds for the operator norm function. Hence, increasing the intensity of the excitation S_0 can be compensated by also increasing the natural frequency ω_f and damping ratio ζ_f of the associated filter to achieve a similar reliability level. Furthermore, Fig. 1 shows that $P_F(\boldsymbol{\theta})$ and $\|\mathbf{M}(\boldsymbol{\theta})\|_{\infty,2}$ are reduced (increased) for lower (higher) values of θ_1 and higher (lower) values of θ_2 . Hence, the failure probability, which quantifies the plausibility of unacceptable structural behavior, and the operator norm, which quantifies the amplification of the vector of basic random variables $\boldsymbol{\xi}$, seem to be reduced for weaker and more damped excitations. Correspondingly, stronger and less damped excitations lead to higher values of these functions. Moreover, Fig. 1 also indicates that $P_F(\boldsymbol{\theta})$ and $\|\mathbf{M}(\boldsymbol{\theta})\|_{\infty,2}$ are minimized for $\theta_1 = 0.8$ and $\theta_2 = 1.2$, while their corresponding maxima are obtained for $\theta_1 = 1.2$ and $\theta_2 = 0.8$. Thus, both functions achieve their extrema at the same values of $\boldsymbol{\theta}$. These aspects highlight the validity of employing the operator norm as a proxy for the failure probability in this example, since both functions present a similar behavior with respect to the interval parameters $\boldsymbol{\theta}$.

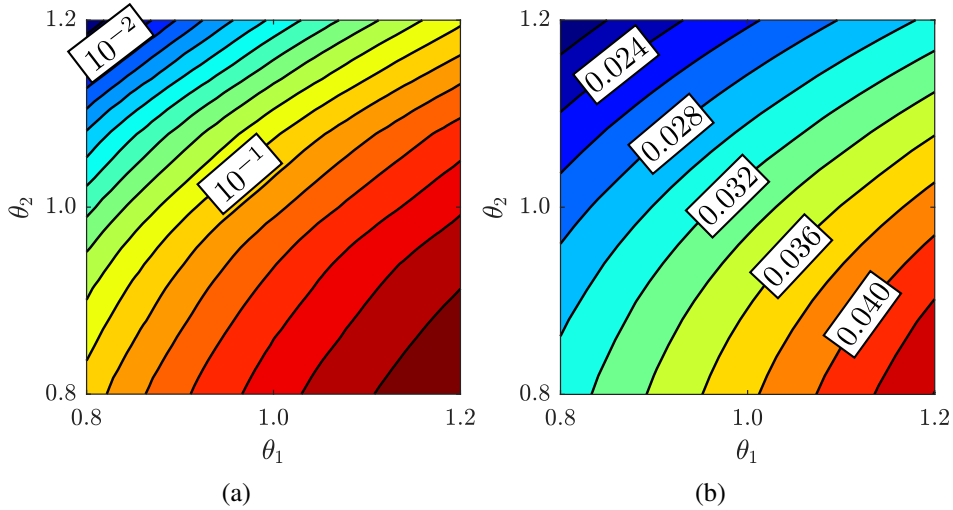


Fig. 1: Contours of the objective functions of a Duffing nonlinear oscillator ($\varepsilon = 2$) with fractional derivative elements ($\alpha = 0.5$): (a) failure probability function $P_F(\boldsymbol{\theta})$, (b) operator norm function $\|\mathbf{M}(\boldsymbol{\theta})\|_{\infty,2}$.

Next, the herein proposed approach is employed to bound the first-passage probability. In this regard, the optimization problems stated in Eqs. (29) and (30) are first solved to determine $\boldsymbol{\theta}^{*,L}$ and $\boldsymbol{\theta}^{*,U}$, respectively. These parameter values, which yield the extrema of the operator norm function $\|\mathbf{M}(\boldsymbol{\theta})\|_{\infty,2}$, are then assumed to determine the extrema of the first-passage probability [17, 19]. Finally, the failure probability function is evaluated at $\boldsymbol{\theta}^{*,L}$ and $\boldsymbol{\theta}^{*,U}$ to estimate the lower and upper bounds of the failure probability according to Eq. (28).

The parameter values obtained by the proposed approach are shown in Table 1, where reference results derived by a standard double-loop implementation are also included for comparison. The corresponding values of the operator norm function, $\|\mathbf{M}(\boldsymbol{\theta})\|_{\infty,2}$, and of the failure probability function, $P_F(\boldsymbol{\theta})$, are also shown in Table 1. It is seen that the minima of the failure probability and operator norm functions are achieved by minimizing θ_1 and maximizing θ_2 , while the corresponding maxima are obtained by maximizing θ_1 and minimizing θ_2 . These results agree with the contours presented in Fig. 1. Moreover, it is noted that the parameter values determined by applying the proposed method are very similar to the corresponding reference results. In fact, due to the inherent variability of sampling-based reliability estimates, the rather small differences observed between the bounds identified by the proposed method and their reference values can be neglected in practice. This highlights the validity of the proposed decoupling strategy, in which a proxy for the failure probability function is developed by integrating the statistical linearization and stochastic averaging methodologies with an operator norm-based solution treatment.

Table 1: Failure probability bounds of a Duffing nonlinear oscillator ($\varepsilon = 2$) with fractional derivative elements ($\alpha = 0.5$) for $n_\theta = 2$; comparison with reference results obtained by a standard double-loop implementation.

	Proposed approach		Reference results	
	P_F^L	P_F^U	P_F^L	P_F^U
θ_1	0.800	1.200	0.800	1.200
θ_2	1.200	0.800	1.200	0.800
$P_F(\boldsymbol{\theta})$	6.54×10^{-3}	4.92×10^{-1}	6.27×10^{-3}	4.94×10^{-1}
$\ \mathbf{M}(\boldsymbol{\theta})\ _{\infty,2}$	2.08×10^{-2}	4.40×10^{-2}	2.08×10^{-2}	4.40×10^{-2}

4.1.2 Case II: Clough-Penzien spectrum with five interval-valued parameters

The case of all user-defined parameters in Eq. (31) characterized as interval-valued and bounded between 80% and 120% of their reference values is considered next. Thus, the excitation model parameters are given by $S_0 = S_0^{\text{ref}}\theta_1$, $\omega_g = \omega_g^{\text{ref}}\theta_2$, $\omega_f = \omega_f^{\text{ref}}\theta_3$, $\zeta_g = \zeta_g^{\text{ref}}\theta_4$, $\zeta_f = \zeta_f^{\text{ref}}\theta_5$, where $\theta_i \in [0.8, 1.2]$, $i = 1, 2, \dots, 5$, are interval variables. In passing, it is noted that the dimension of the vector $\boldsymbol{\theta} \in \Theta$ is higher than the corresponding vector in Section 4.1.1. Therefore, this case can be interpreted as the characterization of a higher degree of uncertainty in terms of the excitation model parameter values.

To study the relationship between the failure probability function and the operator norm function, Fig. 2 presents a scatter plot of $P_F(\boldsymbol{\theta})$ and $\|\mathbf{M}(\boldsymbol{\theta})\|_{\infty,2}$ evaluated at different values of $\boldsymbol{\theta}$. Specifically, 5000 realizations of $\boldsymbol{\theta} \in \Theta$ obtained by means of Latin Hypercube Sampling [55] are considered to generate Fig. 2. Despite the fact that the functional relationship between both quantities is not injective, the results indicate that there is a clear trend between them; that is, higher (lower) values of $\|\mathbf{M}(\boldsymbol{\theta})\|_{\infty,2}$ correspond to higher (lower) values of $P_F(\boldsymbol{\theta})$. Moreover, the average time required to estimate $P_F(\boldsymbol{\theta})$ is roughly 16 times longer than that required to evaluate $\|\mathbf{M}(\boldsymbol{\theta})\|_{\infty,2}$ for the different realizations of $\boldsymbol{\theta}$. The previous outcomes highlight the suitability of the operator norm function as a numerically efficient proxy for the failure probability function in the context of this example.

The results obtained by the proposed approach are presented in Table 2, where reference values obtained by a direct double-loop implementation are also included for comparison. It is readily seen that the herein developed framework for determining the failure probability bounds exhibits a high accuracy degree. Notably, the decoupling strategy presented in Section 3.2 circumvents the repeated evaluation of $P_F(\boldsymbol{\theta})$ at different realizations of $\boldsymbol{\theta}$, thereby requiring only two reliability analyses to estimate such bounds. Furthermore, the model parameter values identified by the developed framework are almost identical to the corresponding reference values. In this regard, and following a similar pattern to the results presented in Table 1, increasing the excitation intensity and reducing the damping levels in Eq. (31) leads to higher values of $P_F(\boldsymbol{\theta})$, whereas weaker and more damped excitations tend to reduce the failure probability level. In addition, the failure probability bounds reported in Table 2 are wider than those determined in Table 1. This outcome is reasonable from a reliability viewpoint, since the dimension of the vector $\boldsymbol{\theta}$ considered in Case II is larger than in Case I. In other words,

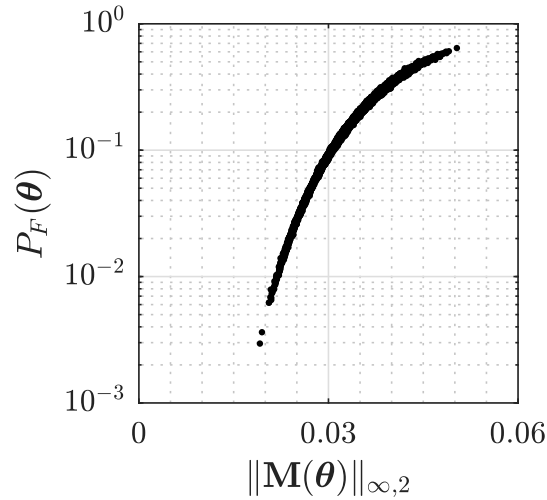


Fig. 2: Failure probability $P_F(\boldsymbol{\theta})$ vs. operator norm $\|\mathbf{M}(\boldsymbol{\theta})\|_{\infty,2}$ of a Duffing non-linear oscillator ($\varepsilon = 2$) with fractional derivative elements ($\alpha = 0.5$) evaluated at different realizations of $\boldsymbol{\theta}$.

Case I can be regarded as a subset of Case II, reinforcing the fact that the probability bounds are wider in the latter case. As anticipated, the herein proposed framework can effectively bound the first-passage probability for the example under consideration.

Table 2: Failure probability bounds of a Duffing nonlinear oscillator ($\varepsilon = 2$) with fractional derivative elements ($\alpha = 0.5$) for $n_\theta = 5$; comparison with reference results obtained by a standard double-loop implementation.

	Proposed approach		Reference results	
	P_F^L	P_F^U	P_F^L	P_F^U
θ_1	0.801	1.199	0.801	1.199
θ_2	0.800	1.186	0.801	1.139
θ_3	1.195	1.169	1.200	1.159
θ_4	1.193	0.802	1.196	0.800
θ_5	1.200	0.800	1.197	0.802
$P_F(\boldsymbol{\theta})$	1.32×10^{-3}	6.81×10^{-1}	1.20×10^{-3}	6.94×10^{-1}
$\ \mathbf{M}(\boldsymbol{\theta})\ _{\infty,2}$	1.75×10^{-2}	5.30×10^{-2}	1.76×10^{-2}	5.31×10^{-2}

4.2 Bilinear hysteretic oscillator with fractional derivative elements

Next, a bilinear hysteretic oscillator with fractional derivative elements is considered. The governing equation of motion is given by Eq. (1) with [20, 56]

$$g(x, \dot{x}) = \gamma\omega_0^2 x(t) + (1 - \gamma)\omega_0^2 x_y z. \quad (36)$$

In Eq. (36), γ denotes the post- to pre-yield stiffness ratio, x_y is the critical value at which yielding occurs, and z is a state variable satisfying

$$x_y \dot{z} = \dot{x} [1 - H(\dot{x})H(z - 1) - H(-\dot{x})H(-z - 1)], \quad (37)$$

where $H(\cdot)$ denotes the Heaviside step function. Considering Eq. (36), Eqs. (15) and (16) become

$$F_1(A) = \begin{cases} \frac{4x_y}{\pi} \left(1 - \frac{x_y}{A}\right), & A > x_y \\ 0, & A \leq x_y \end{cases} \quad (38)$$

and

$$F_2(A) = \begin{cases} \frac{A}{\pi} \left(\Lambda - \frac{1}{2} \sin(2\Lambda)\right), & A > x_y \\ A, & A \leq x_y \end{cases}, \quad (39)$$

respectively, with $\Lambda = \arccos\left(1 - \frac{2x_y}{A}\right)$. Then, considering Eqs. (38) and (39) in conjunction with Eq. (21), Eqs. (17) and (18) yield

$$\begin{aligned} \beta_{eq} = & -\beta_0 + \frac{\beta \sin^2\left(\frac{\alpha\pi}{2}\right)}{\omega_0^{1-\alpha}\sigma^2} \int_0^\infty \frac{A}{\omega^{1-\alpha}(A)} \exp\left(-\frac{\sin\left(\frac{\alpha\pi}{2}\right) A^2}{\omega_0^{1-\alpha} 2\sigma^2}\right) dA \\ & + \frac{4x_y\omega_0^2(1-\gamma) \sin\left(\frac{\alpha\pi}{2}\right)}{\pi\omega_0^{1-\alpha}\sigma^2} \int_{x_y}^\infty \frac{1 - \frac{x_y}{A}}{\omega(A)} \exp\left(-\frac{\sin\left(\frac{\alpha\pi}{2}\right) A^2}{\omega_0^{1-\alpha} 2\sigma^2}\right) dA \end{aligned} \quad (40)$$

and

$$\begin{aligned} \omega_{eq}^2 = & \omega_0^2 - (1 - \gamma)\omega_0^2 \left\{ \exp\left(-\frac{x_y^2 \sin\left(\frac{\alpha\pi}{2}\right)}{2\sigma^2\omega_0^{1-\alpha}}\right) \right. \\ & \left. - \frac{\sin\left(\frac{\alpha\pi}{2}\right)}{\pi\omega_0^{1-\alpha}\sigma^2} \int_{x_y}^\infty \left(\Lambda - \frac{1}{2} \sin(2\Lambda)\right) A \exp\left(-\frac{\sin\left(\frac{\alpha\pi}{2}\right) A^2}{\omega_0^{1-\alpha} 2\sigma^2}\right) dA \right\} \\ & + \frac{\beta \sin\left(\frac{\alpha\pi}{2}\right) \cos\left(\frac{\alpha\pi}{2}\right)}{\omega_0^{1-\alpha}\sigma^2} \int_0^\infty \omega^\alpha(A) A \exp\left(-\frac{\sin\left(\frac{\alpha\pi}{2}\right) A^2}{\omega_0^{1-\alpha} 2\sigma^2}\right) dA, \end{aligned} \quad (41)$$

respectively. Similar to the case examined in Section 4.1, Eqs. (40), (41) and (22) define a coupled system of nonlinear algebraic equations to be solved for determining the equivalent elements β_{eq} and ω_{eq}^2 . To this end, the iterative scheme described in Appendix A is applied.

The values $\alpha = 0.5$, $\omega_0 = 10$ and $\beta = 2\zeta_0\omega_0^{2-\alpha} = 6.32$ with $\zeta_0 = 0.1$ are used for the system parameters in Eq. (1), while in Eq. (36), $\gamma = 0.2$ and $x_y = 0.016$. Finally, the response threshold in Eq. (32) is $x^* = 0.29$.

4.2.1 Determination of first-passage failure probability bounds

It is assumed that all parameters of the stochastic excitation model in Eq. (31) are interval-valued. They are given by $S_0 = S_0^{\text{ref}}\theta_1$, $\omega_g = \omega_g^{\text{ref}}\theta_2$, $\omega_f = \omega_f^{\text{ref}}\theta_3$, $\zeta_g = \zeta_g^{\text{ref}}\theta_4$ and $\zeta_f = \zeta_f^{\text{ref}}\theta_5$, where $\theta_i \in [0.8, 1.2]$, $i = 1, 2, \dots, 5$, are interval variables. That is, each parameter of the excitation model is assumed to be bounded between 80% and 120% of its corresponding reference value.

Subsequently, the first-passage failure probability of the bilinear oscillator defined by Eqs. (1), (36) and (37) is bounded by employing the framework described in Section 3 in conjunction with Eqs. (40) and (41). Table 3 reports the results obtained by the proposed approach, which are compared against reference values determined by a direct double-loop implementation. It is seen that the failure probability bounds obtained by the proposed method are quite similar to their reference values. Moreover, given the inherent variability associated with sampling-based reliability estimates, the bounds estimated by both methods can be regarded as equivalent in practice. In addition, it is seen that the model parameter values that yield the extrema of $P_F(\boldsymbol{\theta})$, which are explicitly identified by the direct double-loop approach under consideration, are very similar to those that determine the extrema of $\|\mathbf{M}(\boldsymbol{\theta})\|_{\infty,2}$, which are explicitly obtained by means of the herein developed framework. Hence, the regions of the parameter space Θ that yield the minimum and maximum values of the operator norm function also seem to provide the minimum and maximum values of the failure probability function, respectively. In this regard, it is noted that the estimation of the first-passage probability bounds by the proposed decoupling approach requires, according to Eq. (28), only two evaluations of the failure probability function. As already pointed out, this feature can yield significant computational savings since it circumvents the repeated evaluation of $P_F(\boldsymbol{\theta})$ at different realizations of $\boldsymbol{\theta}$.

Table 3: Failure probability bounds of a bilinear hysteretic oscillator ($\gamma = 0.2$, $x_y = 0.016$) with fractional derivative elements ($\alpha = 0.5$) for $n_\theta = 5$; comparison with reference results obtained by a standard double-loop implementation.

	Proposed approach		Reference results	
	P_F^L	P_F^U	P_F^L	P_F^U
θ_1	0.800	1.200	0.803	1.199
θ_2	0.802	0.800	0.810	0.810
θ_3	1.200	0.800	1.198	0.801
θ_4	1.200	0.800	1.199	0.809
θ_5	1.199	0.800	1.196	0.802
$P_F(\boldsymbol{\theta})$	2.25×10^{-3}	9.82×10^{-1}	2.00×10^{-3}	9.83×10^{-1}
$\ \mathbf{M}(\boldsymbol{\theta})\ _{\infty,2}$	2.11×10^{-2}	1.61×10^{-1}	2.15×10^{-2}	1.61×10^{-1}

4.2.2 Effect of the fractional derivative order on the first-passage probability bounds

Next, the proposed framework is employed to investigate how the fractional order α affects the first-passage probability bounds. Firstly, the relationship between the operator norm and the failure probability functions is shown in Fig. 3, where scatter plots of $\|\mathbf{M}(\boldsymbol{\theta})\|_{\infty,2}$ vs. $P_F(\boldsymbol{\theta})$ are depicted for various values of the fractional order; namely, for $\alpha = 0.25$, $\alpha = 0.5$ and $\alpha = 0.75$. For each plot, 5000 realizations of $\boldsymbol{\theta} \in \Theta$ were generated with Latin Hypercube Sampling [55]. Note, in passing, that the damping coefficient in Eq. (1) is given by $\beta = 2\zeta_0\omega_0^{2-\alpha}$ with $\zeta_0 = 0.1$. Figure 3 indicates that, despite the non-injective relationship between $P_F(\boldsymbol{\theta})$ and $\|\mathbf{M}(\boldsymbol{\theta})\|_{\infty,2}$, a positive trend between them exists for the considered values of the fractional order. Hence, it is argued that the values of $\boldsymbol{\theta}$ that minimize (maximize) the operator norm function also minimize (maximize) the failure probability function. This also agrees with the results presented in Table 3 and supports the adoption of $\|\mathbf{M}(\boldsymbol{\theta})\|_{\infty,2}$ as a numerically efficient proxy of the failure probability function for the cases under consideration.

Table 4 shows the failure probability bounds obtained by the proposed approach for different values of the fractional order α . It is readily seen that increasing the value of α results in decreasing the failure probability levels for the example under consideration. Such behavior is expected from a structural dynamics viewpoint since, in general, larger values of the fractional order are associated

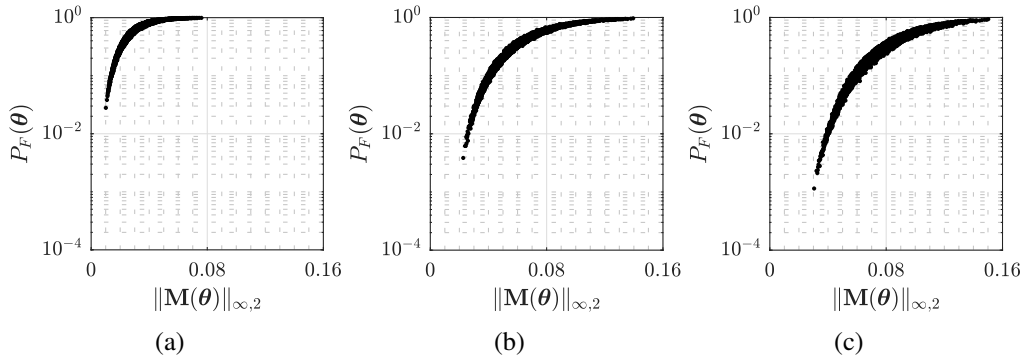


Fig. 3: Failure probability $P_F(\boldsymbol{\theta})$ vs. operator norm $\|\mathbf{M}(\boldsymbol{\theta})\|_{\infty,2}$ of a bilinear hysteretic oscillator ($\gamma = 0.2$, $x_y = 0.016$) with fractional derivative elements evaluated at different realizations of $\boldsymbol{\theta}$: (a) fractional order $\alpha = 0.25$, (b) fractional order $\alpha = 0.5$, (c) fractional order $\alpha = 0.75$.

with greater dissipation levels. This, in turn, may result in a reduction of the magnitude of the response displacement, and thus, shift the probability mass towards smaller response levels. In particular, the lower bound for the failure probability appears more sensitive to the value of α than the corresponding upper bound. For instance, increasing the fractional order from $\alpha = 0.25$ to $\alpha = 0.75$ decreases the value of P_F^U by approximately 3%, whereas the value of P_F^L decreases by (roughly) one order of magnitude. Hence, the value of the fractional order can have a significant impact on the reliability of the considered bilinear hysteretic oscillator with fractional derivative elements. Finally, validation calculations indicate that the bounds shown in Table 4 agree satisfactorily well with reference values obtained from a direct double-loop implementation. These results, as well as the results presented in Tables 2 and 3, highlight the applicability of the herein developed framework, in the sense that it represents a versatile and computationally efficient alternative for bounding the failure probability of a class of nonlinear oscillators endowed with fractional derivative elements and subject to stationary Gaussian excitation.

5 Concluding remarks

In this paper, an approximate analytical technique has been proposed for bounding the first-passage probability of lightly damped nonlinear and hysteretic oscillators endowed with fractional derivative elements, and subjected to imprecise stationary

Table 4: Failure probability bounds of a bilinear hysteretic oscillator ($\gamma = 0.2$, $x_y = 0.016$) with fractional derivative elements for different values of the fractional order α .

Fractional order (α)	Lower bound (P_F^L)	Upper bound (P_F^U)
0.25	1.81×10^{-2}	9.99×10^{-1}
0.50	2.25×10^{-3}	9.82×10^{-1}
0.75	7.16×10^{-4}	9.66×10^{-1}

Gaussian loads. Specifically, the statistical linearization and stochastic averaging methodologies have been integrated with an operator norm-based solution treatment, and a numerically efficient proxy function for the first-passage probability has been established. Then, the first-passage probability function has been evaluated at the parameter values that determine the minimum and maximum of the proposed proxy to approximate the lower and upper bounds of the first-passage probability. A salient feature of the herein developed framework is that each first-passage probability bound is computed in a fully decoupled manner. That is, the repeated evaluation of the failure probability function at different realizations of the interval-valued parameters is effectively circumvented by virtue of the adopted solution treatment. Moreover, it can readily treat a wide range of nonlinear and hysteretic behaviors and can be extended, in principle, to account for non-stationary excitation loads. Overall, the proposed framework can be construed as an extension of a recently developed linearization-based decoupling scheme to account for systems with fractional derivative elements. A hardening Duffing and a bilinear hysteretic nonlinear oscillators with fractional derivative elements subject to imprecise Gaussian loads have been considered in the numerical examples section to assess the efficacy of the proposed framework. Based on comparisons with reference values, it has been shown that the technique represents a versatile and computationally efficient alternative to bound the first-passage probability of a class of nonlinear oscillators subject to stationary Gaussian loads.

Declaration of competing interest

The authors declare that they have no known competing financial interests or personal relationships that could have appeared to influence the work reported in this paper.

Acknowledgments

The authors gratefully acknowledge the support by the German Research Foundation (Grant No. FR 4442/2-1), and by the Hellenic Foundation for Research and Innovation (Grant No. 1261).

Appendix A. Iterative procedure for determining the equivalent linear oscillator

The solution of Eqs. (17), (18) and (22) for a given value of θ , which yields the equivalent linear elements β_{eq} and ω_{eq} in Eq. (19), is carried out by means of the following iterative procedure:

1. Initialize σ_{old}^2 with a small positive value. In this contribution, $\sigma_{old}^2 \leftarrow 10^{-4}$ is considered.
2. Substitute σ_{old}^2 into Eq. (21) to get the response amplitude PDF $p(A)$.
3. Obtain the equivalent linear elements β_{eq} and ω_{eq} by Eqs. (17) and (18), respectively.
4. Use the values of β_{eq} and ω_{eq} obtained in step 3 to evaluate the variance σ_{cand}^2 according to Eq. (22).
5. If $|\sigma_{cand}^2 - \sigma_{old}^2|/\sigma_{old}^2 \leq 10^{-5}$ stop the procedure and retrieve β_{eq} and ω_{eq} . Otherwise, set $\sigma_{old}^2 \leftarrow \sigma_{cand}^2$ and go back to step 2.

References

- [1] Masanobu Shinozuka and Ym Sato. Simulation of nonstationary random process. Journal of the Engineering Mechanics Division, 93(1):11–40, 1967.
- [2] G. M. Atkinson and W. Silva. Stochastic modeling of California ground motions. Bulletin of the Seismological Society of America, 90(2):255–274, apr 2000.
- [3] Ove Ditlevsen. Stochastic model for joint wave and wind loads on offshore structures. Structural Safety, 24(2-4):139–163, apr 2002.

- [4] Jianbing Chen, Yupeng Song, Yongbo Peng, and Pol D. Spanos. Simulation of homogeneous fluctuating wind field in two spatial dimensions via a joint wave number-frequency power spectrum. Journal of Engineering Mechanics, 144(11), 2018.
- [5] Nam Hoang, Yozo Fujino, and Pennung Warnitchai. Optimal tuned mass damper for seismic applications and practical design formulas. Engineering Structures, 30(3):707–715, mar 2008.
- [6] Fernando Gomez and Billie F. Spencer. Topology optimization framework for structures subjected to stationary stochastic dynamic loads. Structural and Multidisciplinary Optimization, 59(3):813–833, sep 2018.
- [7] Cheng Su, Baomu Li, Taicong Chen, and Xihua Dai. Stochastic optimal design of nonlinear viscous dampers for large-scale structures subjected to non-stationary seismic excitations based on dimension-reduced explicit method. Engineering Structures, 175:217–230, nov 2018.
- [8] B. Goller, H. J. Pradlwarter, and G. I. Schuëller. Reliability assessment in structural dynamics. Journal of Sound and Vibration, 332(10):2488–2499, may 2013.
- [9] D. Moens and D. Vandepitte. Recent advances in non-probabilistic approaches for non-deterministic dynamic finite element analysis. Archives of Computational Methods in Engineering, 13(3):389–464, sep 2006.
- [10] Michael Beer, Scott Ferson, and Vladik Kreinovich. Imprecise probabilities in engineering analyses. Mechanical systems and signal processing, 37(1-2):4–29, 2013.
- [11] Matthias Faes and David Moens. Recent trends in the modeling and quantification of non-probabilistic uncertainty. Archives of Computational Methods in Engineering, 27(3):633–671, feb 2019.
- [12] Matthias G. R. Faes, Marco Daub, Stefano Marelli, Edoardo Patelli, and Michael Beer. Engineering analysis with probability boxes: A review on computational methods. Structural Safety, 93:102092, nov 2021.
- [13] Roland Schöbi and Bruno Sudret. Structural reliability analysis for p-boxes using multi-level meta-models. Probabilistic Engineering Mechanics, 48:27–38, apr 2017.

- [14] Pengfei Wei, Jingwen Song, Sifeng Bi, Matteo Broggi, Michael Beer, Zhenzhou Lu, and Zhufeng Yue. Non-intrusive stochastic analysis with parameterized imprecise probability models: I. Performance estimation. Mechanical Systems and Signal Processing, 124:349–368, jun 2019.
- [15] Pengfei Wei, Fuchao Liu, Marcos Valdebenito, and Michael Beer. Bayesian probabilistic propagation of imprecise probabilities with large epistemic uncertainty. Mechanical Systems and Signal Processing, 149:107219, feb 2021.
- [16] Xiukai Yuan, Matthias G. R. Faes, Shaolong Liu, Marcos A. Valdebenito, and Michael Beer. Efficient imprecise reliability analysis using the Augmented Space Integral. Reliability Engineering & System Safety, 210:107477, jun 2021.
- [17] Matthias G R Faes, Marcos A Valdebenito, David Moens, and Michael Beer. Bounding the first excursion probability of linear structures subjected to imprecise stochastic loading. Computers & Structures, 239:106320, 2020.
- [18] Matthias G R Faes, Marcos A Valdebenito, David Moens, and Michael Beer. Operator norm theory as an efficient tool to propagate hybrid uncertainties and calculate imprecise probabilities. Mechanical Systems and Signal Processing, 152:107482, 2021.
- [19] Peihua Ni, Danko J Jerez, Vasileios C Fragkoulis, Matthias G R Faes, Marcos A Valdebenito, and Michael Beer. Operator norm-based statistical linearization to bound the first excursion probability of nonlinear structures subjected to imprecise stochastic loading. ASCE-ASME Journal of Risk and Uncertainty in Engineering Systems, Part A: Civil Engineering, 8(1):04021086, 2022.
- [20] John Brian Roberts and Pol D Spanos. Random vibration and statistical linearization. Courier Corporation, 2003.
- [21] Jocelyn Sabatier, Om Prakash Agrawal, and J. A. Tenreiro Machado, editors. Advances in fractional calculus. Springer Netherlands, 2007.
- [22] Yuriy A Rossikhin and Marina V Shitikova. Application of fractional calculus for dynamic problems of solid mechanics: novel trends and recent results. Applied Mechanics Reviews, 63(1), 2010.

- [23] Mario Di Paola, Antonina Pirrotta, and AJMoM Valenza. Visco-elastic behavior through fractional calculus: an easier method for best fitting experimental results. Mechanics of materials, 43(12):799–806, 2011.
- [24] Isabel S Jesus and JA Tenreiro Machado. Development of fractional order capacitors based on electrolyte processes. Nonlinear Dynamics, 56:45–55, 2009.
- [25] Francesco Paolo Pinnola. Statistical correlation of fractional oscillator response by complex spectral moments and state variable expansion. Communications in Nonlinear Science and Numerical Simulation, 39:343–359, 2016.
- [26] A Pirrotta, I A Kougioumtzoglou, A Di Matteo, V C Fragkoulis, A A Pantelous, and C Adam. Deterministic and random vibration of linear systems with singular parameter matrices and fractional derivative terms. Journal of engineering mechanics, 147(6):04021031, 2021.
- [27] Ioannis A Kougioumtzoglou, Peihua Ni, Ioannis P Mitseas, Vasileios C Fragkoulis, and Michael Beer. An approximate stochastic dynamics approach for design spectrum based response analysis of nonlinear structural systems with fractional derivative elements. International Journal of Non-Linear Mechanics, 146:104178, 2022.
- [28] Yuanjin Zhang, Ioannis A Kougioumtzoglou, and Fan Kong. A Wiener path integral technique for determining the stochastic response of nonlinear oscillators with fractional derivative elements: A constrained variational formulation with free boundaries. Probabilistic Engineering Mechanics, page 103410, 2023.
- [29] Wei Zhang, Pol D Spanos, and Alberto Di Matteo. Nonstationary stochastic response of hysteretic systems endowed with fractional derivative elements. Journal of Applied Mechanics, 90(6):061011, 2023.
- [30] Lincong Chen and Weiqiu Zhu. First passage failure of SDOF nonlinear oscillator with lightly fractional derivative damping under real noise excitations. Probabilistic Engineering Mechanics, 26(2):208–214, 2011.
- [31] Wei Li, Lincong Chen, Natasa Trisovic, Aleksandar Cvetkovic, and Junfeng Zhao. First passage of stochastic fractional derivative systems with power-

- form restoring force. International Journal of Non-Linear Mechanics, 71:83–88, 2015.
- [32] Pol D Spanos, Alberto Di Matteo, Yezeng Cheng, Antonina Pirrotta, and Jie Li. Galerkin scheme-based determination of survival probability of oscillators with fractional derivative elements. Journal of Applied Mechanics, 83(12):121003, 2016.
- [33] Vasileios C Fragkoulis and Ioannis A Kougioumtzoglou. Survival probability determination of nonlinear oscillators with fractional derivative elements under evolutionary stochastic excitation. Probabilistic Engineering Mechanics, page 103411, 2023.
- [34] Yuanjin Zhang, Fan Kong, Shujin Li, and Rongyue Zhu. Survival probability determination of nonlinear oscillators subject to combined deterministic periodic and non-stationary stochastic loads. Mechanical Systems and Signal Processing, 199:110464, 2023.
- [35] J B Roberts and P D Spanos. Stochastic averaging: an approximate method of solving random vibration problems. International Journal of Non-Linear Mechanics, 21(2):111–134, 1986.
- [36] W. Q. Zhu. Recent developments and applications of the stochastic averaging method in random vibration. Applied Mechanics Reviews, 49(10S):S72–S80, oct 1996.
- [37] Vasileios C Fragkoulis, Ioannis A Kougioumtzoglou, and Athanasios A Pantelous. Statistical linearization of nonlinear structural systems with singular matrices. Journal of Engineering Mechanics, 142(9):04016063, 2016.
- [38] A Di Matteo, P D Spanos, and A Pirrotta. Approximate survival probability determination of hysteretic systems with fractional derivative elements. Probabilistic Engineering Mechanics, 54:138–146, 2018.
- [39] Ketson R M dos Santos, Ioannis A Kougioumtzoglou, and Pol D Spanos. Hilbert transform-based stochastic averaging technique for determining the survival probability of nonlinear oscillators. Journal of Engineering Mechanics, 145(10):04019079, 2019.

- [40] Renjie Han, Vasileios C Fragkoulis, Fan Kong, Michael Beer, and Yongbo Peng. Non-stationary response determination of nonlinear systems subjected to combined deterministic and evolutionary stochastic excitations. International Journal of Non-Linear Mechanics, 147:104192, 2022.
- [41] Vasileios C Fragkoulis, Ioannis A Kougioumtzoglou, Athanasios A Pantelous, and Michael Beer. Non-stationary response statistics of nonlinear oscillators with fractional derivative elements under evolutionary stochastic excitation. Nonlinear Dynamics, 97:2291–2303, 2019.
- [42] Ioannis A Kougioumtzoglou and Pol D Spanos. An approximate approach for nonlinear system response determination under evolutionary stochastic excitation. Current science, pages 1203–1211, 2009.
- [43] Wilbur B Davenport and William L Root. An introduction to the theory of random signals and noise, volume 159. McGraw-Hill New York, 1958.
- [44] Polichronis-Thomas D Spanos and Loren D Lutes. Probability of response to evolutionary process. Journal of the Engineering Mechanics Division, 106(2):213–224, 1980.
- [45] Pol D Spanos, Ioannis A Kougioumtzoglou, Ketson R M dos Santos, and André T Beck. Stochastic averaging of nonlinear oscillators: Hilbert transform perspective. Journal of Engineering Mechanics, 144(2):04017173, 2018.
- [46] George Stefanou. The stochastic finite element method: past, present and future. Computer methods in applied mechanics and engineering, 198(9-12):1031–1051, 2009.
- [47] Anil Chopra. Dynamics of structures: Theory and applications to earthquake engineering. Pearson, Hoboken, NJ, 2017.
- [48] Hector A Jensen and Marcos A Valdebenito. Reliability analysis of linear dynamical systems using approximate representations of performance functions. Structural Safety, 29(3):222–237, 2007.
- [49] Lloyd N. Trefethen and David Bau. Numerical linear algebra. Cambridge, 1997.
- [50] Jie Li and Jianbing Chen. Stochastic dynamics of structures. John Wiley & Sons, 2009.

- [51] D. J. Jerez, H. A. Jensen, M. Beer, and J. Chen. Asymptotic Bayesian Optimization: A Markov sampling-based framework for design optimization. Probabilistic Engineering Mechanics, 67:103178, jan 2022.
- [52] Siu-Kui Au and James L. Beck. Estimation of small failure probabilities in high dimensions by subset simulation. Probabilistic Engineering Mechanics, 16(4):263–277, 2001.
- [53] Siu-Kui Au and Yu Wang. Engineering risk assessment with subset simulation. John Wiley & Sons, 2014.
- [54] James C Spall. Introduction to stochastic search and optimization: estimation, simulation, and control. John Wiley & Sons, 2005.
- [55] Thomas J Santner, Brian J Williams, and William I Notz. The design and analysis of computer experiments, volume 1. Springer, 2003.
- [56] T. K. Caughey. Random excitation of a system with bilinear hysteresis. Journal of Applied Mechanics, 27(4):649–652, dec 1960.